Hydrol. Earth Syst. Sci. Discuss., 12, 9765–9811, 2015
www.hydrol-earth-syst-sci-discuss.net/12/9765/2015/
doi:10.5194/hessd-12-9765-2015

Hydrology and Earth System Sciences
Discussions
Open Access

Stochastic or statistic? Comparing flow duration curve models in ungauged basins and changing climates

M. F. Müller and S. E. Thompson

Department of Civil and Environmental Engineering, Davis Hall, University of California, Berkeley CA, USA

Received: 22 August 2015 – Accepted: 31 August 2015 – Published: 25 September 2015

Correspondence to: M. F. Müller (marc.f.muller@gmail.com)

Published by Copernicus Publications on behalf of the European Geosciences Union.

Abstract

The prediction of flow duration curves (FDCs) in ungauged basins remains an important task for hydrologists given the practical relevance of FDCs for water management and infrastructure design. Predicting FDCs in ungauged basins typically requires spatial interpolation of statistical or model parameters. This task is complicated if climate becomes non-stationary, as the prediction challenge now also requires extrapolation through time. In this context, process-based models for FDCs that mechanistically link the streamflow distribution to climate and landscape factors may have an advantage over purely statistical methods to predict FDCs.

This study compares a stochastic (process-based) and statistical method for FDC prediction in both stationary and non-stationary contexts, using Nepal as a case study. Under contemporary conditions, both models perform well in predicting FDCs, with Nash–Sutcliffe coefficients above 0.80 in 75 % of the tested catchments. The main drives of uncertainty differ between the models: parameter interpolation was the main source of error for the statistical model, while violations of the assumptions of the process-based model represented the main source of its error. The process-based approach performed better than the statistical approach in numerical simulations with non-stationary climate drivers. The predictions of the statistical method under non-stationary rainfall conditions were poor if (i) local runoff coefficients were not accurately determined from the gauge network, or (ii) streamflow variability was strongly affected by changes in rainfall. A Monte Carlo analysis shows that the streamflow regimes in catchments characterized by a strong wet-season runoff and a rapid, strongly non-linear hydrologic response are particularly sensitive to changes in rainfall statistics. In these cases, process-based prediction approaches are strongly favored over statistical models.

HESSD

12, 9765–9811, 2015

FDC Predictions in ungauged basins

M. F. Müller and S. E. Thompson

1 Introduction

The flow duration curve (FDC) provides a compact summary of the variability of daily streamflow by indicating what proportion of the flow regime exceeds a given flow rate. FDCs have considerable practical relevance, particularly in supporting decisions that are affected by the availability and reliability of surface water. Common applications of FDCs include the design and management of hydropower infrastructure (e.g., Basso and Botter, 2012; Müller et al., 2015), the determination of environmental flow standards for ecosystem protection (e.g., Lazzaro et al., 2013) and the allocation of water resources for consumptive uses (e.g., Alaouze, 1989).

Despite their utility, empirical FDCs are unavailable for many basins, primarily because they require extensive on-site observations of daily streamflow (Vogel and Fennessey, 1994). Globally, the preponderance of catchments remain ungauged (or the gauge data that exist are subject to significant quality assurance and data availability constraints). Furthermore, the global number of stream gauges continues to decline because of ongoing budgetary constraints faced by water monitoring agencies (Stokstad, 1999; United States Geological Survey, 2015). Therefore FDCs must typically be estimated in data-scarce areas. The most widely used techniques for FDC estimation are simple, graphical methods. Such empirical methods are easy to implement but often rely on overly simplistic assumptions that lead to substantial prediction errors. For instance in Nepal, the regionalization method prescribed in official design manuals (e.g., Chitrakar, 2004; Alternative Energy Promotion Center, 2014) relies on *one* in-situ observation of streamflow during the dry season to scale standardized regional indices for monthly flows. The procedure neglects the inter-annual variability of low-flows, which leads to important biases in the predicted flow distributions (see Appendix A). Even in gauged catchments, FDCs constructed from historical observations may not represent current flow conditions well, because flow regimes are impacted by climate change and anthropogenic alterations of the catchments (e.g. Botter et al., 2013; Mu et al., 2007). Predicting streamflow in

HESSD
12, 9765–9811, 2015

ungauged basins, particularly in the context of environmental change, remains both a fundamental necessity for water managers and a major research challenge (Blöschl et al., 2013; Montanari et al., 2013).

Recent efforts to predict FDCs in ungauged catchments focus on statistical approaches that predict the flow distribution based on the catchment's similarity to nearby, gauged watersheds (Castellarin et al., 2013). Index flow approaches, which regionalize specific index flows (typically the mean flow), and use those indices to rescale empirical FDCs from similar catchments, are particularly popular (e.g., Chalise et al., 2003; Castellarin et al., 2004b; Sauquet and Catalogne, 2011; Arora et al., 2005). While differing in methodological details, all index flow approaches assume that FDCs do not vary within homogeneous regions, except by a scaling factor. Because they do not assume any specific runoff-generating process, statistical methods are versatile. They have been successfully been applied globally to predict FDCs in a variety of climates and catchment types (Blöschl et al., 2013). However, methods are also insensitive to the diversity of controls on the shape of the FDC exerted by climate processes and catchment characteristics. This may affect their reliability under non-stationary conditions (Milly et al., 2008). Finally, the calibration of statistical methods relies on extensive streamflow observations from a large number of representative and well characterized catchments (e.g., Cheng et al., 2012; Coopersmith et al., 2012). Their performance is therefore sensitive to the spatial density of available gauges Blöschl et al. (2013), and their reliability in regions where streamflow data is truly scarce is uncertain.

Stochastic, process-based models that mechanistically link the drivers, state and response of the system are a promising avenue to address these issues. In these models, basic assumptions about the stochastic structure of rainfall and the (deterministic) response of catchments allow the analytic derivation of streamflow probability density functions (PDFs). (Note that because the FDC can be obtained directly by transforming the PDF, a predictive technique that yields the streamflow PDF will also allow the FDC to be estimated). Botter et al. (2007b) show that runoff follows a gamma distribution if catchments behave as a linear reservoir, forced by stochastic rainfall that follows a marked Poisson process. The resulting gamma distribution depends on two parameters that are determined by the recession characteristics of the catchment, and by the frequency and intensity of effective rain. This process-based approach to the streamflow PDF has been extended to include the fast flow component of streamflow (Muneepeerakul et al., 2010), non-linearities in subsurface storage–runoff relationships (Botter et al., 2009), the effects of short-term snowmelt (Schaefli et al., 2013) and the carryover of subsurface storage between seasons in seasonally dry climates (Müller et al., 2014). Although the stochastic framework allows the effects of changes in climate or landscape to be independently modeled, it relies on strong simplifying assumptions about the spatial homogeneity of catchments, and it is most appropriate for catchments where streamflow is routed through a shallow water table. These assumptions makes the existing process models less versatile than statistical methods. Nonetheless, the approach has low calibration requirements because it relies on a small number of parameters, which can be determined using rainfall, climate and geomorphological characteristics of the catchments (Doulatyari et al., 2015). This information is increasingly available in ungauged basins, thanks to remote-sensing technologies, even when ground-based measurements are sparse.

Process-based models successfully reproduce streamflow PDFs in numerous catchments worldwide (Botter et al., 2007a; Ceola et al., 2010; Müller et al., 2014). A recent cross-validation analysis (Castellarin et al., 2013) suggested that process-based approaches were less accurate than statistical approaches for predicting FDCs in ungauged catchments. However, the same study noted the sensitivity of index flow methods to the density of available stream gauges. The two approaches are yet to be compared in regions where the local gauge density is globally representative (as opposed to the densely monitored French and Austrian catchments considered by Castellarin et al., 2013). For lower gauge densities, it is unclear whether the advantages of the process-based approaches, which are derived from an explicit representation of flow-generating processes, are outweighted by the limitations imposed by the restrictive

HESSD
12, 9765–9811, 2015

M. F. Müller and S. E. Thompson

assumptions underlying these methods – and whether this trade-off is altered by non-stationarity in climate drivers.

Using Nepal as a test case, this study compares the process-based and statistical approaches on the basis of (i) their ability to predict FDCs in ungauged basins, (ii) their sensitivity to data-scarcity, represented both by the spatial density of the stream gauge network and by thetemporal extent (length) of the available streamflow records, and (iii) their ability to accommodate changes in the rainfall regime.

Nepal provides an ideal setting to compare the two approaches, for four reasons. First, the country is representative of global availability of streamflow data, as measured by the density of its stream gauge network (Fig. 1a). Second, methods drawn from both statistical and process-based approaches have been developed and validated in Nepal. Here we compare the stochastic-dynamic framework developed in Müller et al. (2014), with the index flow model described in Chalise et al. (2003). Third, flow generation processes in Nepalese Himalayan catchments are complex, particularly with respect to the spatial and temporal properties of precipitation. Rainfall derives from the Indian Summer Monsoon and is strongly affected by topography. As a result, local rainfall is temporally autocorrelated, spatially heterogeneous and highly seasonal. There is also significant carryover of groundwater storage between the wet and dry seasons, so that dry season discharge reflects the features of the antecedent wet season. These characteristics violate many of the assumptions that underlie the process-based method. The analysis in Nepal is therefore likely to provide a conservative estimate of the potential performance of the process-based method in ungauged basins. Finally, developing reliable methods for FDC prediction in Nepal represents an opportunity for "use-inspired science" (Thompson et al., 2013b). Nepal has an enormous untapped hydropower potential and is in dire need of electrical power, particularly in rural areas. A reliable method to estimate FDCs in ungauged catchments would be a valuable tool to support the development of micro hydropower, a sustainable technology for rural electrification (Müller et al., 2015).

HESSD
12, 9765–9811, 2015

M. F. Müller and S. E. Thompson

Section 2 describes the two models and the procedures used to estimate their parameters from streamflow and rainfall observations. Section 3 presents the results of the comparative analysis in Nepal. Section 4 examines the key sources of errors for both models and discusses implications for both Prediction in Ungauged Catchments (PUB) and Predictions Under Change (PUC) beyond Nepal.

2 Methods

2.1 Compared approaches

2.1.1 Process-based model

The process-based approach models daily streamflow as a random variable. Subject to strong simplifying assumptions about rainfall stochasticity and runoff generation, the streamflow PDF can be analytically derived. During the wet season, daily rainfall is represented as a stationary marked Poisson process with exponentially distributed depths. Assuming linear evapotranspiration losses, Botter et al. (2007b) showed that effective rain, that is the portion of the total rainfall that contributes to streamflow generation, also follows a stationary marked Poisson process. For a spatially homogenous catchments with an exponentially distributed response time (i.e. a catchment that behaves as a linear reservoir), this effective rainfall will produce gamma-distributed streamflow. The parameters of the gamma distribution are derived from the frequency (λ_P) and mean depth (α_P) of rainfall, and from the recession constant (k) of the catchment. If rainfall in the dry season is sufficiently minimal that effective rainfall does not contribute to runoff generation, then dry season streamflow represents only the discharge of groundwater stored during the previous wet season. This discharge is modeled as a single seasonal recession with stochastic initial conditions that depend on the wet season properties. Because groundwater is not replenished during the dry season, the water table is subject to a large transient

HESSD
12, 9765–9811, 2015
FDC Predictions in ungauged basins
M. F. Müller and S. E. Thompson

drawdown, resulting in a nonlinear discharge behavior and a power law relation between recession rate and discharge (Brutsaert and Nieber, 1977). We showed in Müller et al. (2014) that the distribution of streamflow, and therefore the FDC, in seasonally dry climates that meet the assumptions above can be expressed analytically as a function of seven independent parameters: the frequency (λ_P) and mean intensity (α_P) of wet season rainfall, maximum daily evapotranspiration during the wet season (ET), the water storage capacity of the soil in the root zone (SSC), the (linear) wet-season recession constant (k), the duration of the dry season (T_d) and the exponent of the power law recession during the dry season (b). The formal derivation of the model is summarized in Appendix B.

Three of the seven parameters of the model (T_d, λ_P, α_P) are rainfall characteristics that can be estimated in ungauged basins using meteorological observations. Recession parameters (k and b) describe aquifer properties that are challenging to observe at the catchment scale. They can be estimated using observed streamflow time series in nearby gauged basins, and subsequently interpolated from nearby gauges, using the geostatistical approach described in Müller and Thompson (2015), which accounts for the topology of the stream network. The last two parameters (ET) and (SSC) describe catchment-scale soil moisture dynamics that are arduous to determine empirically. Previous applications of the model relied on reasonable values of ET and SSC, based on land use, soil and climate characteristics of the catchment (e.g., Botter et al., 2007a; Ceola et al., 2010). Alternatively, runoff coefficients can be used to directly relate rainfall statistics to streamflow increments (Doulatyari et al., 2015). Runoff coefficients describe the ratio of mean discharge to mean precipitation, and can be predicted in ungauged basins using water balance models and meteorological observations. This approach circumvents the need to estimate ET and SSC, but the accuracy of predicted runoff coefficients in ungauged catchment is critically dependent on the type of water balance model used and on the availability of appropriate calibration data (Doulatyari et al., 2015). Instead, this study follows the former procedure and uses reasonable estimates of ET and SSC for Nepal.

HESSD
12, 9765–9811, 2015

2.1.2 Statistical model

The statistical approach is entirely driven by observation data and does not assume any specific runoff generation process. Instead, it identifies and exploits statistical correlations that may occur between streamflow observed at existing gauges and the geology, topography and climate of the corresponding catchments. The index flow model used in this study was developed by Chalise et al. (2003) to regionalize FDCs in Nepal to assess the potential for small hydropower development. The model is based on local flow indices for mean ($Q_m = E[Q]$) and low flows ($q_{95} = Q_{95}/Q_m$, where Q_{95} is the 95th streamflow percentile) and uses a non-parametric approach to represent the shape of the FDC. Empirical FDCs from available gauges are normalized by Q_m and pooled into equally-sized groups based on the q_{95} index of the gauge. A standardized curve is determined for each group by taking the average of the normalized flows corresponding to each duration, in order to represent the average catchment response in the group.

Predictions in ungauged catchments are obtained by first using linear regressions to predict Q_m and q_{95}. Although the original method calls for a stepwise multiple regressions approach to determine regression covariates inductively, we used the regression models obtained in Chalise et al. (2003): Q_m is regressed against annual rainfall (R_y) and gauge elevation (z_{min}) as a proxy for evapotranspiration; and q_{95} is regressed against the ratios of catchment area occupied by each of the considered geological units. The two regressions loosely represent the long term water balance and short-term response of the catchment. The predicted low-flow index is then used to determine the standardized FDC shape, which is finally multiplied by the predicted mean flow to obtain the FDC. An important assumption, inherent to the linear regression models, is that the dependent variable (here Q_m and q_{95}) is not autocorrelated, when controlling for the considered covariates. This assumption is reasonable in Nepal, where the typical distance between stream gauges is much larger than the correlation scale of runoff (Müller and Thompson, 2015). In more

HESSD
12, 9765–9811, 2015

M. F. Müller and S. E. Thompson

densely gauged areas (or if runoff is correlated over larger distances), streamflow observations at neighboring or flow-connected gauges are likely to be correlated. In these regions, accounting for the effect of distance and stream network topology when interpolating flow indices (e.g., using TopREML; Müller and Thompson, 2015) will improve predictions.

2.2 Study region and data

The two methods were evaluated using observed streamflow data from 25 Nepalese catchments mapped in Fig. 1b. The gauges in this dataset (HKH-FRIEND, 2004; Department of Hydrology and Meteorology, 2011) have at least 10 years of daily streamflow records. They were checked for consistency, using double mass plots (Searcy and Hardison, 1960), and bias: we discarded non-glaciated catchments that had a precipitation deficit on their long term water balance. Watersheds were delineated using the ASTER GDEM v2 digital elevation model (NASA Land Processes Distributed Active Archive Center, LP DAAC). The study watersheds are located in central Nepal but cover a wide variety of catchment sizes, elevation ranges, precipitation characteristics and geological units (Table 1).

We focused on the Chepe Kohla catchment in central Nepal (Fig. 1b, insert) as a case study for analyses requiring resampling (Sect. 2.3.1) or simulation (Sect. 2.3.2) of streamflow time series. The Chepe Kohla watershed has a long (by Nepalese standards) record of daily streamflow observations (31 years) and is representative of the full sample of gauges in terms of topography and recession behavior (Table 1). The catchment is also small (i.e. close to spatially homogenous) and local rainfall is well approximated by a marked Poisson process (AR = 0.09, CV = 1.09), echoing the underlying assumptions of the process-based model.

Rainfall characteristics over the sampled catchments were obtained from 178 precipitation gauges (HKH-FRIEND, 2004; Department of Hydrology and Meteorology, 2011), also mapped on Fig. 1b. The average duration of the dry season (T_d) was estimated at each precipitation gauge by fitting a step function to the corresponding rainfall time series (Müller and Thompson, 2013), and wet-season precipitation records were used to compute the frequency and mean intensity of rainfall (λ_P and α_P). Rainfall characteristics were then aggregated at the catchment level by assuming that the rain process aggregates linearly within the basins. For rainfall occurence, we assumed that the duration between rain events caused by two consecutive storms can be estimated as the average of the inter-arrival times measured at the rain gauges within the catchment. This allows us to compute catchment level rainfall frequency as:

$$\lambda_\mathrm{P} = \left(\frac{1}{N_\mathrm{g}} \sum_i^{N_\mathrm{g}} \lambda_\mathrm{P}^{(i)} \right)^{-1}$$

where $\lambda_\mathrm{P}^{(i)}$ designates rainfall frequency observed at gauge i and N_g the number of rain gauges within the catchment. Similarly, the catchment-level duration between rainy seasons is assumed to be the average of the durations observed within the catchment:

$$T_\mathrm{d} = \frac{1}{N_\mathrm{g}} \sum_i^{N_\mathrm{g}} T_\mathrm{d}^{(i)}$$

Finally, the precipitation depth received on any given day by a catchment is assumed to be the average of the precipitation depths observed by individual rain gauges. It follows that the aggregated mean rainfall intensity can be expressed as:

$$\alpha_\mathrm{P} = \lambda_\mathrm{P}^{-1} \frac{1}{N_\mathrm{g}} \sum_i^{N_\mathrm{g}} \lambda_\mathrm{P}^{(i)} \alpha_\mathrm{P}^{(i)}$$

If no precipitation station is located within the catchment, rainfall characteristics observed at the rain station closest to the catchment centroid were considered. The chosen procedure was preferred over the alternate approach of aggregating daily rainfall observations at the catchment level *before* computing rainfall characteristics, for two reasons. Firstly, the chosen procedure does not require overlapping rainfall observation periods. Secondly, and more importantly, the frequency and intensity of catchment-aggregated rainfall are strongly affected by the relation between the size of the catchment, the spatial heterogeneity of rainfall and the density of available rain gauges. In Nepal, where monsoon rainfall events are frequent and local, it may rain somewhere within a large catchment every day of the wet season, yet many local storms do not result in streamflow responses at the catchment outlet. For instance, in the 12 000 km^2 Behri catchment in Western Nepal, a rainfall frequency of 1 is obtained when aggregating daily rainfall observations during the wet season. Runoff events are predicted to occur with a frequency of 0.93 when accounting for soil moisture dynamics (Eq. B1), which overestimates frequency of streamflow increases actually observed at the catchment outlet by 100 %.

Recession characteristics were estimated using streamflow observations as described in Müller et al. (2014). We computed wet season recession constants (k) by regressing the logarithm of streamflow against time for each period of consecutively decreasing streamflow during the wet season. The recession constant was then obtained by taking the median value of the regression coefficients of recessions lasting more than four days. The power law exponent of dry season recessions (b) was obtained by fitting a non-linear recession curve

$$Q(t) = (Q_0^{1-b} - a(1-b)t)^{\frac{1}{1-b}} \tag{1}$$

to base flow, which was computed from observed streamflow time series using the Lyne Hollick algorithm (Nathan and McMahon, 1990). The last streamflow peak of the wet season was taken as initial flow condition Q_0, and we used a stochastic optimization algorithm (Simulated Annealing, Bélisle, 1992) to minimize least square fitting errors. In ungauged catchments, the scale exponent of the seasonal recession

HESSD
12, 9765–9811, 2015

was approximated as (Müller et al., 2014):

$$a \approx \frac{\lambda}{-r}\left(e^{\frac{-r}{m}} - 1\right)(\alpha_Q \cdot (m+1)), \quad (2)$$

where $r = 1 - b$; m is the ratio between the frequency λ of effective rain events and the linear recession constant k, and α_Q is the average depth of effective rain events (see Appendix B).

Potential evapotranspiration was approximated by applying the empirical relation estimated by Lambert and Chitrakar (1989) for Nepal during the rainy season (July–September):

$$\mathrm{ET} \approx 4.0 - 0.0008 \cdot z_{\mathrm{mean}}$$

where ET is given in [$\mathrm{mm\,d^{-1}}$] and z_{mean} is the average elevation of the catchment in meters. The formula provides daily average evapotranspiration estimates for each month. It accounts for elevation but assumes a spatially homogenous elevation gradient. A uniform soil moisture capacity of 50 mm was assumed throughout the country, based on empirical observations reported in Shrestha (1997). By neglecting local *variation in* soil characteristics, this produces conservative estimates of the performance of the process-based model in ungauged basins.

2.3 Comparative analyses

2.3.1 Predictions in ungauged basins

We used three cross-validation techniques to evaluate the predictive ability of both methods in ungauged basins. Firstly, a leave-one-out analysis was carried out to assess predictive performances in a realistic situation, where FDCs are predicted in Nepal using all streamflow gauges available in the region. Secondly, we examined the sensitivity of the methods to decreasing data-availability by reducing the number

HESSD
12, 9765–9811, 2015

M. F. Müller and S. E. Thompson

of gauges available to calibrate the models. Finally, we performed a similar data-degradation procedure, but in this case we reduced the number of daily streamflow observations, while holding the number of gauges constant. This final analysis accounts for the challenges posed by recent or temporary installation of stream gauges, which introduce uncertainties into the estimation of model parameters due to the short streamflow records used. These errors can propagate through the model and affect the prediction of FDCs.

In a leave-one-out analysis, one gauge is “left out” of the dataset, and streamflow is predicted at the “missing” location using observations from the remaining gauges. The predicted FDC is then compared to observations from the omitted gauge. The resulting error between observation and prediction yields the prediction performance of the method at that catchment if it were not gauged. Repeating the procedure for all gauges offers an approximation to the overall prediction error of the method. To measure this error we constructed error duration curves (Müller et al., 2014), where the relative prediction error at each flow quantile is plotted against the corresponding duration. Error duration curves allow the partitioning of prediction errors across flow quantiles to be visualized. General prediction performances (across all durations) at individual gauges were also determined using the Nash–Sutcliffe coefficient (NSC) on log streamflow quantiles (Müller et al., 2014):

$$\mathrm{NSC} = 1 \frac{\sum_{t=1}^{364}\left(\ln Q_t^{(\mathrm{emp})} - \ln Q_t^{(\mathrm{mod})}\right)^2}{\sum_{t=1}^{364}\left(\ln Q_t^{(\mathrm{emp})} - E[\ln Q_t^{(\mathrm{emp})}]\right)^2} \tag{3}$$

where $Q_t^{(\mathrm{emp})}$ and $Q_t^{(\mathrm{mod})}$ are the empirical and modeled streamflow quantile of duration t.

The effect of the number of calibration gauges was assessed using a jack-knife cross-validation analysis (Shao and Tu, 2012; Müller and Thompson, 2013). At each of 10 000 iterations, a selected fraction of the available gauges was randomly sampled

HESSD
12, 9765–9811, 2015

(without replacement) and used to predict the FDC at one (randomly selected) remaining gauge. Prediction accuracies for flow duration curves (given by the NSC) and uncertainties on the spatial interpolation of model parameters were reported for each iteration. The procedure was repeated for decreasing numbers of selected "training" gauges.

The available streamflow data did not allow a direct evaluation of the effects of timeseries length through cross-validation, because such an analysis requires substantial overlaps in the monitoring periods of all gauges. Therefore we focused the final analysis on the Chepe Kohla catchment which has the longest observation record in our dataset. We evaluated the effect of the length of the available observation records on parameter estimation, and propagated the ensuing uncertainty in the parameters to the FDCs predicted by each model. To do this, we selected a fixed number of full years of streamflow observations, estimated the parameters, predicted the FDC using these parameters, and compared the results to the empirical FDC obtained from the full observation record. The procedure was repeated 10 000 times. The estimation errors in the model parameters and the resulting FDC prediction performances (NSC) were recorded as a function of the number of sampled years. This analysis is not intended to describe the models' ability to predict FDCs at catchments with short observation records: in this case, constructing an empirical FDC using the available (however short) observation record is likely to be the best course of action (Castellarin et al., 2004a). Instead, the analysis is intended to simulate the effect of short observation records on FDC prediction at nearby, *ungauged* catchments. The underlying assumptions behind this analysis are that (i) the error associated with interpolation is independent of the stream record length, and (ii) the Chepe Kohla catchment is representative of Nepalese basins.

2.3.2 Predictions under change

We used numerical simulations to assess the ability of both models to predict streamflow when subject to changing rainfall regimes.

HESSD
12, 9765–9811, 2015

Synthetic streamflow time series were generated by coupling the stochastic rainfall generator described in Müller and Thompson (2013) and a rainfall–runoff model that simulates the streamflow generating processes described in Sect. 2.1.1. The generated rainfall is a first order Markov process (i.e. rainfall occurrence on a given day is correlated to rainfall occurrence on the previous day) with gamma-distributed rainfall intensities. The duration of the rainy season was assumed constant, and no rainfall was generated during the dry season. These assumptions are close to the observed reality in Nepal, as seen in Fig. 4a, where the FDC constructed from the simulated streamflow is a close approximation to the empirical FDC in the Chepe Kohla watershed.

We translated the effect of shifts in precipitation regimes into changed streamflow for the Chepe Kohla catchment by considering a range of future combinations for rainfall frequencies and intensities. In line with what is expected in Nepal (Turner and Slingo, 2009; Turner and Annamalai, 2012), we considered negative changes in the frequency and positive changes in the mean daily rainfall depth. We neglected changes in soil moisture capacity, evapotranspiration, rainfall autocorrelation and the duration of the rainy season. These parameters are explicit in the process-based model, so we expect differences in the sensitivity of the process and statistical models to climate change to be underestimated by this procedure.

For each rainfall scenario, we evaluated the performance of the models in a changing climate by generating 1000 years of daily streamflow using future rainfall frequencies and intensities. We compared the resulting synthetic FDC to model predictions using *future* rainfall conditions, but using recession and low flow parameters that were determined from *current* streamflow conditions.

Two contrasting cases were considered for the statistical model, depending on the causal validity of the estimated relation between annual precipitation and average streamflow. The statistical model estimates this relation with linear regression over a cross-sectional sample of catchments, which have a variety of unobserved characteristics that may affect both the average flow and annual rainfall (e.g., local topographic features). As a result, the estimated regression coefficients may be biased (omitted variable bias, Greene, 2003) and not representative of the true (causal) relation between mean rainfall and mean flow. The extent of this bias cannot be quantified a priori, so we considered the two extreme cases of zero and infinite biases. The former (zero bias) represents the case where regression coefficients perfectly describe the effect of annual rainfall on average flow. Therefore, assuming future rainfall conditions are known, the future flow conditions can be perfectly estimated. We model this situation by estimating Q_m directly from the (simulated) *future* flow conditions. Conversely, if no effective relationship can be determined between rainfall and mean flow, then the best estimator of future mena flow is the *current* flow condition. For both cases, q_{95} was determined from current flow conditions. Prediction performances (NSC) were plotted against the relative change in the frequency and intensity of rainfall, and compared to the performance of the process-based model.

3 Results

3.1 Prediction in ungauged basins

Results from the leave-one-out cross-validation analysis are presented in Fig. 2 and show that both methods perform similarly in the prediction of FDCs in ungauged basins. Error duration curves (Fig. 2a and b) show comparable streamflow prediction uncertainties: 75 % of the predicted flow quantiles are between half and double the observed streamflow for both models, although the low flows in the process-based model display an increasing upwards bias (Fig. 2b). Considering the Nash–Sutcliffe coefficients computed at the individual basin level, the mean and median performances are again comparable for both models, but the accuracy of the statistical model predictions are more variable across sites than the process model predictions, as indicated by the larger spread of the Nash–Sutcliffe coefficients (Fig. 2c).

Figure 3a (top) shows prediction performances of both models as the number of streamflow gauges available for predictions decreases, and indicates that the

HESSD
12, 9765–9811, 2015

performance of both models is relatively insensitive to the gauge density, until it declines to less than approximately 0.6 gauges per 10 000 km^2. For such situations, which represent discarding more than half the available gauges in Nepal, the statistical model performance declines rapidly compared to the process-based model. Prediction performances are strongly affected by uncertainties on the interpolation of model parameters, as seen in Fig. 3a (bottom). Interpolation uncertainties are generally larger for the flow indices of the statistical model (Q_m and q_{95}) than for the recession parameters of the process-based model (k and b). This explains the larger spread in prediction performances of the former (Fig. 2c and error bars in Fig. 3a, top). The parameter uncertainties are also relatively insensitive to the total gauge density until about 60 % of the originally available gauges are discarded. At this point, the uncertainties associated with estimation of the flow indices increase significantly, while the process-based model parameters remain more reasonably estimated.

When considering short observation windows, parameter uncertainties also drive the performance of the models. Figure 3b (top) shows the prediction performance of both models at the Chepe Khola watershed, as the number of observation years used to estimate the model parameters is reduced. In this case, the statistical model outperforms the process-based model when less than 10 years of streamflow observations are available. The parameter uncertainties associated with the short timeseries estimates (Fig. 3b, bottom) suggest that a longer time series of streamflow observations is needed to accurately estimate the wet-season parameter (k), resulting in the lower performance of the process-based model for short streamflow records.

3.2 Prediction under change

Simulation results presented in Fig. 4b show both models' ability to predict a simulated future flow duration curve of the Chepe Kohla River, under a range of different possible changes in rainfall regimes. In all simulations, parameters describing the hydrological response of the basin (k, b, and q_{95}) are determined using current flow conditions, and evapotranspiration is assumed constant. The results show that explicitly modeling

HESSD
12, 9765–9811, 2015

rainfall–runoff processes allows the process-based model to accommodate the effects of the changing precipitation regime. In contrast, the performance of the statistical model is affected at various degrees by shifts in rainfall regimes, depending on how the model translates changes in annual precipitations to changes in average flows. If these shifts are perfectly represented by the model, then prediction errors arise solely from changes in the shape of the FDC, and the process and statistical models perform similarly in the Chepe Kohla watershed across the full range of considered rainfall scenarios (Fig. 4b, dashed curve). If, however, average (future) streamflows cannot be reliably predicted from the predicted changes in annual rainfall, the statistical model does not accommodate flow regime changes at all. Future FDCs are modeled using current streamflow observations, and the ensuing prediction errors can be significant (Fig. 4b, dotted curve). The simulated cases provide upper and lower bounds for the actual performance of the statistical model in future rainfall regimes. We evaluated the model's ability to predict Q_m by using cross sectional data (i.e. average streamflow and annual rainfall from the 25 catchments) to estimate the linear relation between Q_m and annual rainfall R_y. Applied to the Chepe Kohla watershed, the estimated regression coefficients allowed the annual streamflow to be estimated from annual precipitation with a bias of −13 % and a coefficient of determination of $R^2 = 0.57$ (Fig. 4c). Regardless, prediction errors remained negligible for both bounds (NSC > 0.95) for the range of changes actually anticipated in Nepal (e.g., $\Delta\lambda_\mathrm{P}/\lambda_\mathrm{P} \approx 0.98$ and $\Delta\alpha_\mathrm{P}/\alpha_\mathrm{P} \approx 1.20$ for the $2 \cdot CO_2$ scenario; Turner and Slingo, 2009).

4 Discussion

4.1 Predictions in ungauged basins

The analysis suggests that both statistical and process-based methods to estimate FDCs in ungauged basins perform comparably in Nepal, over a wide range of gauge densities and observation durations. Yet prediction performances varied significantly

HESSD
12, 9765–9811, 2015

M. F. Müller and S. E. Thompson

between the models as data became increasingly sparse. The statistical method is more sensitive to spatially sparse data, which degrades the interpolation accuracy of Q_m. In contrast, the process-based method is more sensitive to temporally restricted observations, which reduce the accuracy with which recession parameters can be estimated. This suggests that the performance of the two models in ungauged basins is affected by different sources of uncertainty. In this section, we investigate the source of prediction error in each methods and discuss the implications for their application in ungauged basins beyond Nepal.

4.1.1 Sources of uncertainty in the statistical model

The statistical model relies on two assumptions about the correlations of observed data. First, it assumes that the flow indices (Q_m and q_{95}) at ungauged catchments can be best predicted using linear regressions against observable covariates (annual rainfall, elevation and geology). This assumption does not hold if the flow indices are spatially auto-correlated, or if the posited linear relations are spatially heterogeneous or, in fact, non-linear. Further, "omitted variable" biases (Greene, 2003) will arise if an unobserved variable is correlated to both a covariate and a flow index. For instance, local topographic features may affect both the annual rainfall and the average streamflow in mountainous regions. This leads to substantial uncertainty in the interpolation of the flow indices in Nepal.

This interpolation, indeed, is the main source of prediction errors in FDCs, as shown in Fig. 5d. Using observed (instead of predicted) flow indices substantially reduces the width of the error-duration curve of the statistical method. The relative sensitivity of the statistical method to interpolation errors in each flow index was evaluated through a numerical simulations (Fig. 6a). The prediction performance was more sensitive to errors in Q_m than q_{95}. This is consistent with the fact that, while Q_m has a direct effect on all the quantiles of the FDC, q_{95} only determines the type of FDC shape that is selected, and two different values of q_{95} may generate identical FDC shapes.

HESSD
12, 9765–9811, 2015
FDC Predictions in ungauged basins
M. F. Müller and S. E. Thompson

The second assumption is that catchments with similar low-flow indices (q_{95}) have identical hydrological responses, and therefore identical FDC shapes. Errors caused by the violation of this assumption appear in the error duration curve on Fig. 5a. The statistical method assigns gauges to a finite number of bins, according to their low flow index, and determines a FDC shape for each bin. The error duration curve shown on Fig. 5a represents differences in the FDC shapes of catchments within the bins (i.e. with similar low flow indices). A tradeoff arises in determining the number of bins: a small number of large bins leads to large averaging errors within the bins, while a large number of thin bins increases the model's sensitivity to interpolation errors in q_{95}.

4.1.2 Sources of uncertainty in the process-based model

In contrast, interpolation uncertainties on the model parameters (k and b) only marginally affect the prediction performance of the process-based approach (Fig. 5a). Instead, two sources of error appear to drive prediction performance. Firstly, uncertainties are caused by the aggregation of point-rainfall statistics to the catchment level (see Sect. 2.2). These errors are caused by spatial heterogeneities in wet season rainfall and principally affect high flows, as seen when comparing Figs. 5b and c. They can be mitigated by improved rainfall data, which are increasingly available in many regions, as rainfall observation satellite missions proliferate and improve. Unfortunately, orographic rainfall in mountainous regions remains challenging to quantify from space-borne platforms. In Nepal, current remote sensing precipitation products (e.g., TRMM 3B42) are substantially biased and do not outperform available rain gauges in predicting the frequency and intensity of areal rainfall (Müller and Thompson, 2013).

A second source of error arises from the simplifying assumptions made about flow processes, which do not hold perfectly in the observed catchments. While the model is remarkably robust to deviations from key assumptions on rainfall distribution and recession relations (see Müller et al., 2014), prediction errors at low flows appear to

HESSD
12, 9765–9811, 2015

be caused by errors in the determination of a, the scale parameter of the non-linear seasonal recession (Fig. 5b). The process-based model assumes that, because they describe the same watershed, the wet and dry recession parameters are physically related. In Müller et al. (2014), a is expressed as an explicit function of k and b for sufficiently short recession times, where power-law recessions can be approximated by exponential functions. Although this approach provides more accurate estimates of a than would be obtained through spatial interpolation (Fig. 5e), estimation uncertainties remain, propagate through the model and drive prediction errors during the dry season.

The numerical analysis presented in Fig. 6 illustrates the crucial importance of dry-season recession constants. Unlike the statistical model, the process-based model is affected by errors in both of its parameters (k and b). However, the model's sensitivity to k drops if the wet-season recession constant is *not* used to determine a, as seen in Fig. 6c, where the error introduced on k does not propagate to a. This effect is also visible in the resampling analysis on short time series (Fig. 3c), where the uncertainty on k only marginally affects prediction performance, which declines when b estimates become inaccurate. This shows that the performance of the model is strongly driven by the estimation of dry-season recession constants in ungauged catchments.

4.1.3 Applicability beyond Nepal

Fundamentally, the statistical model relies on observed correlations, rather than assumptions about hydrologic mechanisms. Because FDC shapes are modeled non-parametrically, the approach is applicable to regions with highly variable catchment responses. However, prediction performance in ungauged basins is constrained by interpolation errors in the mean flow. This makes the method unsuitable for regions where the local determinants of mean flow (i.e. rainfall, evapotranspiration, glacial melt) cannot be accurately monitored at the catchment level. In contrast, a key advantage of the process-based model is its ability to exploit characteristics of the stochastic structure of rainfall that can be estimated from daily rainfall observations. The model is appropriate for regions where the spatial heterogeneity of runoff is driven by rainfall,

HESSD
12, 9765–9811, 2015

and where the frequency and intensity of rainfall depths at the catchment level can be readily estimated (i.e. small catchments with numerous rain gauges, or places where satellite observations provide a good representation of rainfall statistics). Unlike rainfall, recession behavior arises from lumped and complex interactions between climate, vegetation and groundwater processes that typically cannot be monitored in a spatially explicit manner. The process-based model is therefore inappropriate for regions where the hydrologic response of the catchment is the main source of runoff heterogeneity, or where the assumed recession behavior (in particular the relation between a, k and b) does not occur.

Conveniently, the appropriate implementation contexts for both methods appear to be complementary, and the optimal method in a given region is determined by the driving source of runoff heterogeneity in the catchments. Ultimately, the performance of both methods is constrained by their ability to estimate their parameters in ungauged basins. This relation is apparent in Fig. 3, where drops in prediction performances correspond to increases in the estimation uncertainty of model parameters. Under these conditions, the performance of each method is driven by the ability of the available observations to capture the variability of the model parameters. When interpolated from neighboring gauges, uncertainties are governed by the interplay between the layout of the gauges and the spatial correlation range of the considered model parameter. When estimated from short observation records, accuracy is determined by the extent to which the available record is representative of the temporal variability of the parameter. These interactions between data availability and runoff variability are inherently local and will affect the determination of the most appropriate method for any given region.

4.2 Prediction under change

Expected shifts in the frequency and intensity of Monsoon rainfall over Nepal only have a marginal impact on the streamflow distributions in the Chepe Kohla catchment, as shown by the numerical simulation presented in (Fig. 4a, dashed curve). Consequently, changes in rainfall regime do not appear to affect the performance of either model

HESSD
12, 9765–9811, 2015
FDC Predictions in ungauged basins

M. F. Müller and S. E. Thompson

(Fig. 4b), unless they are significantly larger then expected. Climate change may nonetheless affect flow predictions elsewhere. In this section, we investigate the conditions under which FDCs can be reliably predicted in a changing climate. We discuss the vulnerabilities of the prediction models to non-stationary rainfall, and characterize the resilience of stream flow regimes in relation to observable catchment attributes.

4.2.1 Resilience of prediction models

Although rainfall stationarity is an inherent assumption of the process-based approach, climate change can be incorporated by updating the relevant parameters to their future value to predict the (pseudo-)stationary future state of the system. The method accounts for otherwise confounding changes in the frequency and intensity of rainfall, which are expected in Nepal. By explicitly accounting for soil moisture dynamics and recession behavior, the model emulates the (causal) effect of rainfall on streamflow. As a result, the method reliably predicts the distribution of future streamflow, provided that governing flow generation processes are in line with the basic assumptions listed in Sect. 2.1.1.

In contrast, the statistical model is solely based on observed correlations, leading to two important sources of errors for predictions under change. First, the model only accommodates rainfall changes to the extent that the estimated statistical relation between rainfall and runoff is representative of local runoff coefficients. The model will not reliably predict future streamflows if runoff coefficients are strongly spatially heterogeneous, or if the cross sectional sample of gauges fails to capture important processes governing mean flow. This source of uncertainty appears to be significant in Nepal, as illustrated by the substantial bias in annual flow predictions on Fig. 4c. Secondly, the statistical model only considers the effect of *average* rainfall on *average* flow: the effect of rainfall *distribution* in streamflow *distribution* is ignored. As a result, the model cannot predict changes in the shape of FDC that are brought about by changing rainfall. The prediction performance of the statistical approach is therefore

HESSD
12, 9765–9811, 2015

M. F. Müller and S. E. Thompson

determined by the resilience of the flow regime, that is the extent to which streamflow distribution is affected by shifting rain signals: the method will perform poorly in catchments with a poorly resilient flow regimes.

4.2.2 Resilience of flow regimes in seasonally dry climates

We examine the linkages between the resilience of flow regimes and the physical characteristics of the catchments. This allows us to identify regions, where the statistical method may not provide reliable predictions under change because flow distribution is is vulnerable to changing rainfall. By explicitly representing runoff generation processes, the stochastic dynamic framework used in the process-based model is an ideal tool to explore the resilience of flow regimes in catchments that follow its basic underlying assumptions (Sect. 2.1.1). A similar model was used in Botter et al. (2013) to relate the resilience of non-seasonal flow regimes to observable catchment characteristics. Here we discuss the case of seasonally-dry climates, where the characteristics of the seasonal recessions can substantially affect streamflow resilience. We use the relations derived stochastic-dynamic framework (Appendix B) to infer the effect of rainfall and recession characteristics on the resilience of flow regimes, and therefore on the reliability of the statistical model for predictions under change.

During the wet season, the stochastic dynamic framework indicates that flow regimes are determined by the ratio between λ, the frequency of effective (i.e. runoff-generating) rain events, and k the (linear) recession constant that represents the time scale of the hydrological response of the catchment (Botter et al., 2013). If $\lambda/k > 1$, frequent effective rainfall and a slow catchment response guarantee a persistent supply of runoff to the stream. If $\lambda/k < 1$, effective rain is not frequent enough to compensate for rapid decreases in streamflow after runoff events, and the stream may become intermittent. Streamflow in persistent regimes ($\lambda/k > 1$) is driven by rainfall, whereas streamflow in sporadic regimes ($\lambda/k < 1$) is constrained by the ability of the catchment to modulate the release of water stored in the subsurface. Accordingly, rainfall changes affect most flow quantiles in the persistent regime and shift the entire flow distribution, but they

HESSD
12, 9765–9811, 2015

M. F. Müller and S. E. Thompson

preferentially affect high flows in the sporadic regime, which occur immediately after effective rain events. As a result, sporadic regimes are more resilient to climate change in terms of the mean effect on the entire streamflow distribution, as observed by Botter et al. (2013) and illustrated in Fig. 4d. However, when specifically considering climate effects on the *shape* of the flow distribution (i.e. by normalizing all flow quantiles by their mean), sporadic regimes are more vulnerable to rainfall changes, which "tilt" normalized FDCs by preferentially affecting high flows (Fig. 4e). Consequently, we expect the statistical method to perform better in persistent flow regimes because the shape of streamflow distribution is less sensitive to changing rainfall. This is confirmed in the Monte Carlo analysis presented in Appendix C, where the ratio λ/k is positively correlated to the performance of the statistical model.

If no significant rainfall occurs outside of the wet season, climate change only affects dry-season flow through its effect on the initial condition of the seasonal recession. It follows the flow regime will be more sensitive to rainfall changes if the duration of the wet season (when rainfall has a "direct" effect on streamflow) is long. This effect is also visible in the Monte Carlo analysis, where the duration of the wet season (T_w) is negatively associated with the performance of the statistical model.

The extent to which changes in the initial condition affect the shape of the seasonal recession during the dry season is determined by the non-linear character of the catchment's response. This can be seen by using the characteristic time-scale of the recession (here we consider the time necessary to reduce peak flow by $1/e$) to characterize its shape. In linear catchments, the recession takes an exponential form, so the characteristic timescale corresponds to the inverse of the recession constant and is not affected by initial conditions. For non-linear catchments, characteristic time can be derived from Eq. (1):

$$t_{1/e} = \frac{\left(1 - e^{-r}\right) Q_0^r}{ar} \tag{4}$$

with $r = 1 - b$. In these nonlinear regimes, the initial conditions Q_0 clearly have an effect on the shape of the recession of non-linear catchment. Taking the derivative of Eq. (4)

with respect to Q_0 shows that a change in initial flow has a stronger influence on the shape of the recession for low values of Q_0, as illustrated in Fig. 4f. Consequently, the sensitivity of the dry season flow regimes to climate change scenarios is expected to be highest in strongly non-linear catchments with limited wet season runoff. Predictions of the FDC using the statistical model for non-stationary rainfall regimes are likely to be poor. In Monte Carlo analysis (Appendix C), the performance of the statistical method is significantly worse in strongly non-linear catchments. However, the negative correlation between the linearity of the runoff behavior and the prediction performance is weaker for catchments with high wet-season runoff.

The streamflow resilience in seasonally dry catchments depends on two distinct seasonal effects: a "direct" effect driven by the ratio between λ_P and k during the wet season, and an "indirect" effect during the dry season, when resilience is determined by the interplay between Q_0 (i.e. wet-season rainfall) and b. Streamflow resilience influences the ability of the statistical method to predict FDCs under change. In seasonally dry climates, we expect the statistical method to be most reliable in regions where wet seasons are short with limited total rainfall but persistent flow regimes, and where the recession behavior during the dry-season is close to linear.

5 Conclusions

Stochastic, process-based models predicted the FDCs for ungauged catchments in Nepal well, with a performance that was comparable to that of statistical models. It suggests that in regions with globally representative gauge-densities, and under seasonally dry climates, the advantages of the statistical approaches relative to stochastic models noted in previous analyses (Blöschl et al., 2013) no longer apply. The discrepancy between these results and previous studies likely derives from the relative robustness of the interpolation of the stochastic model parameters under sparsely gauged conditions. The complementarity between the different sources of uncertainty in the stochastic and statistical methods suggests that model selection

HESSD
12, 9765–9811, 2015

should be driven by a consideration of the main drivers of heterogeneity in any study catchment: process-based models are advisable if climate is likely to be the main source of runoff heterogeneity. Conversely, statistical methods are more appropriate for regions with substantially different recession behaviors across catchments. These distinctions provide a potentially robust basis for model selection in any given prediction application.

The results also suggest that the sensitivity of statistical approaches to changes in rainfall statistics is dependent on the "resilience" of the flow regime as defined by Botter et al. (2013). Overall, the process-based models are more reliable in projecting FDCs into new rainfall regimes. This is particularly true for catchments characterized by a strong wet-season runoff and a rapid, strongly non-linear hydrologic response, because their flow regime is particularly vulnerable to rainfall changes, making the assumptions of the statistical model inappropriate.

The excellent performance of both process-based and statistical models for the FDC and PDF in ungauged basins suggests that extending probabilistic analyses in such basins to also include flow-derived variables such as hydropower capacity (Basso and Botter, 2012) or ecological responses (Thompson et al., 2013a) may be feasible. While these prospects are enticing, we note that a model's ability to predict an FDC with high fidelity is not necessarily indicative of prediction performances on all derived stochastic properties. For instance, Dralle et al. (2015) demonstrate that the crossing properties of streamflow can be very poorly estimated by stochastic process-based models, even in applications where the same models predict the PDF of flow well. Further exploration of the potential opportunities and limitations afforded by use of probabilistic models in ungauged basins offers a promising avenue for future study.

HESSD
12, 9765–9811, 2015

Appendix A: Performance of the Medium Irrigation Project method in ungauged Nepalese basins

We assess the predictive performance of the Medium Irrigation Project, an empirical method currently used to predict streamflow distribution in small mountainous catchments in Nepal for infrastructure design purposes. The method is prescribed by official micro hydropower design guidelines in Nepal Alternative Energy Promotion Center (2014). The approach, described in Chitrakar (2004), divides Nepal into seven hydrologic regions characterized by different sets of monthly flow indices. Streamflow distribution in ungauged catchments is determined by performing a site visit in mid-April to evaluate discharge under low-flow conditions. In our validation analysis, we emulated this step by selecting the daily flow measured on 15 April of a randomly drawn observation year at each gauge. The measured flow is then used to scale the regional monthly indices corresponding to the location of the catchment. All regions have an index of 1 for the month of April (when low-flow conditions are observed), and larger indices for the other months. FDCs can finally be computed by reordering daily flow values interpolated from the obtained monthly flows.

A fundamental flaw of the method is that it assumes that discharge measured in mid-April on a given year is representative of lowest flow conditions that can be observed in the catchment. This assumption does not hold if effective rain events have occurred shortly before discharge was measured or, more to the point, if the current year is not a particularly dry year. As a result, predicted FDCs substantially overestimate observed flows, as shown in Fig. 5f.

Appendix B: Process-based streamflow distribution model for seasonally dry climates

This appendix presents the analytical expression of FDC in seasonal climates derived in Müller et al. (2014). The approach assumes that rainfall can be represented as

Discussion Paper | Discussion Paper | Discussion Paper | Discussion Paper |

HESSD

12, 9765–9811, 2015

FDC Predictions in ungauged basins

M. F. Müller and S. E. Thompson

Title Page | Abstract | Introduction | Conclusions | References | Tables | Figures | Back | Close | Full Screen / Esc | Printer-friendly Version | Interactive Discussion

a marked Poisson process with with exponentially distributed depths. Catchments are modeled as spatially homogenous linear reservoirs with linear evapotranspiration losses. Under these conditions, wet season streamflow can be represented as a gamma-distributed random variable (Botter et al., 2007b):

$$Q_\mathrm{w} \sim \mathrm{Gamma}(m, \alpha_Q^{-1})$$

with $m = \lambda/k$ and $\alpha_Q = \alpha_\mathrm{P} k A$, and where k is the linear recession constant, A the area of the contributing catchment and α_P the mean intensity of wet season rainfall. The frequency λ of runoff events can be expressed as a function of the frequency (λ_P) and intensity of rainfall (Botter et al., 2007b):

$$\lambda = \eta \frac{\exp(-\gamma)\gamma^{\frac{\lambda_\mathrm{P}}{\eta}}}{\Gamma_L\left(\lambda_\mathrm{P}/\eta, \gamma\right)} \tag{B1}$$

where $\Gamma_L(\cdot,\cdot)$ is the lower incomplete gamma function, and where $\eta = \mathrm{ET}/\mathrm{SSC}$ and $\gamma = \mathrm{SSC}/\alpha_\mathrm{P}$ are respectively the ratio between maximum evapotranspiration and soil storage capacity, and the ratio between soil storage capacity and mean rainfall intensity.

Dry season streamflow is modeled as a seasonal recession starting at the last discharge peak of the wet season. Because wet season streamflow is a gamma-distributed variable, streamflow at discharge peaks, and therefore the initial condition of the seasonal recession, is itself a gamma distributed variable (Müller et al., 2014):

$$Q_\mathrm{peak} \sim \mathrm{Gamma}(m+1, \alpha_Q^{-1}).$$

Assuming a power law-relation between discharge and recession rate, the cumulative distribution function of dry season streamflow can be expressed as (Müller et al., 2014):

$$P_{Q_\mathrm{d}}(Q) = \begin{cases} 1 + \frac{q_\mathrm{d}^r \Gamma_1 - \alpha_Q^r \Gamma_2}{arT_\mathrm{d}\Gamma(m+1)}, & \text{if } Q > -(arT_\mathrm{d})^{\frac{1}{r}} \text{ and } r < 0 \\ 1 + \frac{q_\mathrm{d}^r \Gamma_1 - \alpha_Q^r \Gamma_2}{arT_\mathrm{d}\Gamma(m+1)} + \frac{\alpha_Q^r \Gamma_4 + (Q^r - arT_\mathrm{d})\Gamma_3}{arT_\mathrm{d}\Gamma(m+1)}, & \text{otherwise} \end{cases}$$

Discussion Paper | Discussion Paper | Discussion Paper | Discussion Paper |

HESSD
12, 9765–9811, 2015

FDC Predictions in ungauged basins

M. F. Müller and S. E. Thompson

Title Page
Abstract Introduction
Conclusions References
Tables Figures
◀ ▶
Back Close
Full Screen / Esc
Printer-friendly Version
Interactive Discussion

with

$$\Gamma_1 = \Gamma_\mathrm{U}\left(m+1, \alpha_Q^{-1} Q\right)$$
$$\Gamma_2 = \Gamma_\mathrm{U}\left(r+m+1, \alpha_Q^{-1} Q\right)$$
$$\Gamma_3 = \Gamma_\mathrm{U}\left(m+1, \alpha_Q^{-1} (Q^r + arT_\mathrm{d})^{\frac{1}{r}}\right)$$
$$\Gamma_4 = \Gamma_\mathrm{U}\left(r+m+1, \alpha_Q^{-1} (Q^r + arT_\mathrm{d})^{\frac{1}{r}}\right)$$

$\Gamma(\cdot)$ and $\Gamma_\mathrm{U}(\cdot,\cdot)$ denote the complete and upper incomplete gamma functions; T_d is the duration of the dry season; $r = 1 - b$ and a are the parameters of the non-linear recession, which are assumed stationary. Because they describe the same watershed, recession parameters for the wet and dry seasons are related. If power-law recessions can be approximated by an exponential function for sufficiently short recession times, we can express a as a function of k and b (Müller et al., 2014):

$$a \approx \frac{\lambda}{-r}\left(e^{\frac{-r}{m}} - 1\right)(\alpha_Q \cdot (m+1)) \tag{B2}$$

The law of total probability can finally be used to combine seasonal streamflow distributions and derive the cumulative distribution function of streamflow for the whole year:

$$P_Q(Q) = \left(1 - \frac{T_\mathrm{d}}{365}\right) \cdot P_{Q_\mathrm{w}}(Q) + \frac{T_\mathrm{d}}{365} \cdot P_{Q_\mathrm{d}}(Q) \tag{B3}$$

The FDC for seasonally dry climates is finally obtained by plotting the streamflow quantiles Q against $1 - P_Q(Q)$, the complement of the the cumulative distribution function of streamflow.

HESSD
12, 9765–9811, 2015

Appendix C: Monte Carlo analysis of flow regime resilience

We used a Monte Carlo analysis on numerically generated streamflow to estimate the effect of catchment characteristics on streamflow resilience. In the context of this paper, the resilience of flow regimes to climate change is defined as the robustness of the *shape* of FDCs to shifts in the frequency and intensity of rainfall. The analysis proceeds as follows:

1. Topographic and hydroclimatic characteristics are drawn from uniform distributions as described in Table 2.

2. 1000 years of "current" synthetic daily streamflows are generated from the drawn parameters using the stochastic rainfall generator and rainfall–runoff model described in Sect. 2.3.2.

3. Randomly drawn multiplicative biases are inserted to the parameters representing frequency and intensity of rainfall (λ_P and α_P) to emulate climate change, and 1000 years of "future" synthetic daily streamflow are generated.

4. Current and future FDCs are constructed empirically from the simulated time series, and normalized by their respective means.

5. Differences in the shape of the flow distributions are quantified by computing the Nash–Sutcliffe coefficient on the (log) flow quantiles of the two normalized FDCs.

We repeated the procedure 5000 times and used linear regressions to estimate the effect of catchment characteristics on the resilience of flow regimes, as represented by the Nash–Sutcliffe coefficient.

Ordinary least squares estimates of the considered regression models are presented in Table 3. The first column presents direct correlations between catchment characteristics and flow regime resilience and indicate significant positive effects for rainfall frequency and intensity and a negative effect of both recession constants.

HESSD
12, 9765–9811, 2015

Regression models shown in columns 2 and 3 test the relations hypothesized in the discussions. As expected, column 2 shows that the λ/k ratio has a positive significant effect on the resilience of flow regimes. In order to avoid colinearity issues, all variables used to construct λ (i.e. λ_P and α_P in Eq. B1) where removed from the regression model. The significant negative effect of T_w on streamflow resilience is consistant with the fact that dry season precipitations are neglected. Consequently, changes in rainfall have a direct effect on wet season flows, while only affecting dry season flows through their effect on the initial conditions of the seasonal recession. Lastly, we use mean wet-season rainfall ($\lambda_P\alpha_P$) as a proxy for the initial conditions of the seasonal recession and assess the effect of its interaction with b on flow resilience in column 3. As expected, b is strongly negatively associated to flow resilience but its interaction with $\lambda_P\alpha_P$ is significantly positive. This is consistent with our hypothesis that the shape of non-linear recessions is more vulnerable to climate change, especially if the initial flow conditions are low.

Acknowledgements. The Swiss National Science Foundation are gratefully acknowledged for funding (M. F. Müller).

References

Alaouze, C. M.: Reservoir releases to uses with different reliability requirements, AWRA Water Resour. Bull., 25, 1163–1168, 1989. 9767

Alternative Energy Promotion Center: Construction and Installation Manual for Micro Hydropower Project Installers, Government of Nepal, 2014 (in Nepalese). 9767, 9793

Arora, M., Goel, N., Singh, P., and Singh, R.: Regional flow duration curve for a Himalayan river Chenab, Nord. Hydrol., 36, 193–206, 2005. 9768

Basso, S. and Botter, G.: Streamflow variability and optimal capacity of run-of-river hydropower plants, Water Resour. Res., 48, W10527, doi:10.1029/2012WR012017, 2012. 9767, 9792

Bélisle, C. J.: Convergence theorems for a class of simulated annealing algorithms on Rd, J. Appl. Probab., 29, 885–895, 1992. 9776

HESSD

12, 9765–9811, 2015

FDC Predictions in ungauged basins

M. F. Müller and S. E. Thompson

Blöschl, G., Sivapalan, M., Wagener, T., Viglione, A., and Savenije, H.: Runoff Prediction in Ungauged Basins: Synthesis across Processes, Places and Scales, Cambridge University Press, 2013. 9768, 9791

Botter, G., Peratoner, F., Porporato, A., Rodriguez-Iturbe, I., and Rinaldo, A.: Signatures of large-scale soil moisture dynamics on streamflow statistics across U.S. climate regimes, Water Resour. Res., 43, W11413, doi:10.1029/2007WR006162, 2007a. 9769, 9772

Botter, G., Porporato, A., Rodriguez-Iturbe, I., and Rinaldo, A.: Basin-scale soil moisture dynamics and the probabilistic characterization of carrier hydrologic flows: slow, leachingprone components of the hydrologic response, Water Resour. Res., 43, W02417, doi:10.1029/2006WR005043, 2007b. 9768, 9771, 9794

Botter, G., Porporato, A., Rodriguez-Iturbe, I., and Rinaldo, A.: Nonlinear storage–discharge relations and catchment streamflow regimes, Water Resour. Res., 45, W10427, doi:10.1029/2008WR007658, 2009. 9769

Botter, G., Basso, S., Rodriguez-Iturbe, I., and Rinaldo, A.: Resilience of river flow regimes, P. Natl. Acad. Sci. USA, 110, 12925–12930, doi:10.1073/pnas.1311920110, 2013. 9767, 9789, 9790, 9792

Brutsaert, W. and Nieber, J. L.: Regionalized drought flow hydrographs from a mature glaciated plateau, Water Resour. Res., 13, 637–643, doi:10.1029/WR013i003p00637, 1977. 9772

Castellarin, A., Galeati, G., Brandimarte, L., Montanari, A., and Brath, A.: Regional flow-duration curves: reliability for ungauged basins, Adv. Water Resour., 27, 953–965, doi:10.1016/j.advwatres.2004.08.005, 2004a. 9779

Castellarin, A., Vogel, R., and Brath, A.: A stochastic index flow model of flow duration curves, Water Resour. Res., 40, W03104, doi:10.1029/2003WR002524, 2004b. 9768

Castellarin, A., Botter, G., Hughes, D., Liu, S., Ouarda, T., Parajka, J., Post, D., Sivapalan, M., Spence, C., Viglione, A., and Vogel, R.: Prediction of flow duration curves in ungauged basins, chapt. 7, in: Runoff Prediction in Ungauged Basins: Synthesis Across Processes, Places and Scales, edited by: Blöschl, G., Sivapalan, M., Wagener, T., Viglione, A., and Savenije, H., Cambridge University Press, 135–162, 2013. 9768, 9769

Ceola, S., Botter, G., Bertuzzo, E., Porporato, A., Rodriguez-Iturbe, I., and Rinaldo, A.: Comparative study of ecohydrological streamflow probability distributions, Water Resour. Res., 46, W09502, doi:10.1029/2010WR009102, 2010. 9769, 9772

Chalise, S., Kansakar, S., Rees, G., Croker, K., and Zaidman, M.: Management of water resources and low flow estimation for the Himalayan basins of Nepal, J. Hydrol., 282, 25–35, doi:10.1016/S0022-1694(03)00250-6, 2003. 9768, 9770, 9773

Cheng, L., Yaeger, M., Viglione, A., Coopersmith, E., Ye, S., and Sivapalan, M.: Exploring the physical controls of regional patterns of flow duration curves – Part 1: Insights from statistical analyses, Hydrol. Earth Syst. Sci., 16, 4435–4446, doi:10.5194/hess-16-4435-2012, 2012. 9768

Chitrakar, P.: Micro-Hydropower Design Aids Manual, Small Hydropower Promotion Project (GTZ) and Mini-Grid Support Program, Alternate Energy Promotion Center, Government of Nepal, 2004. 9767, 9793

Coopersmith, E., Yaeger, M. A., Ye, S., Cheng, L., and Sivapalan, M.: Exploring the physical controls of regional patterns of flow duration curves – Part 3: A catchment classification system based on regime curve indicators, Hydrol. Earth Syst. Sci., 16, 4467–4482, doi:10.5194/hess-16-4467-2012, 2012. 9768

Department of Hydrology and Meteorology: Daily Streamflow and Precipitation Data, Kathmandu, 2011. 9774

Doulatyari, B., Betterle, A., Basso, S., Biswal, B., Schirmer, M., and Botter, G.: Predicting streamflow distributions and flow duration curves from landscape and climate, Adv. Water Resour., 83, 285–298, doi:10.1016/j.advwatres.2015.06.013, 2015. 9769, 9772

Dralle, D. N., Karst, N., and Thompson, S.: Dry season streamflow persistence in seasonal climates, Water Resour. Res., in revision, 2015. 9792

Global Runoff Data Center: Global Runoff Data Base, Global Runoff Data Centre, Koblenz, Federal Institute of Hydrology (BfG), 2014. 9805

Greene, W. H.: Econometric Analysis, Prentice Hall, Upper Saddle River, NJ, 2003. 9781, 9784

HKH-FRIEND: Hindu Kush Himalayan – Flow Regimes from International Experimental and Network Data, UNESCO International Hydrological Programme, UNESCO Paris, France, 2004. 9774

Lambert, L. and Chitrakar, B.: Variation of potential evapotranspiration with elevation in Nepal, Mt. Res. Dev., 9, 145–152, 1989. 9777, 9802

Lazzaro, G., Basso, S., Schirmer, M., and Botter, G.: Water management strategies for run-of-river power plants: profitability and hydrologic impact between the intake and the outflow, Water Resour. Res., 49, 8285–8298, doi:10.1002/2013WR014210, 2013. 9767

Milly, P., Julio, B., Malin, F., Robert, M., Zbigniew, W., Dennis, P., and Ronald, J.: Stationarity is dead, Science, 319, 573–574, doi:10.1126/science.1151915, 2008. 9768

Montanari, A., Young, G., Savenije, H., Hughes, D., Wagener, T., Ren, L., Koutsoyiannis, D., Cudennec, C., Toth, E., and Grimaldi, S.: Panta Rhei – Everything Flows: Change in hydrology and society – the IAHS Scientific Decade 2013–2022, Hydrolog. Sci. J., 58, 1256–1275, doi:10.1080/02626667.2013.809088, 2013. 9768

Mu, X., Zhang, L., McVicar, T. R., Chille, B., and Gau, P.: Analysis of the impact of conservation measures on stream flow regime in catchments of the Loess Plateau, China, Hydrol. Process., 21, 2124–2134, doi:10.1002/hyp.6391, 2007. 9767

Müller, M. F. and Thompson, S. E.: Bias adjustment of satellite rainfall data through stochastic modeling: methods development and application to Nepal, Adv. Water Resour., 60, 121–134, doi:10.1016/j.advwatres.2013.08.004, 2013. 9775, 9778, 9780, 9785

Müller, M. F. and Thompson, S. E.: TopREML: a topological restricted maximum likelihood approach to regionalize trended runoff signatures in stream networks, Hydrol. Earth Syst. Sci., 19, 2925–2942, doi:10.5194/hess-19-2925-2015, 2015. 9772, 9773, 9774

Müller, M. F., Dralle, D. N., and Thompson, S. E.: Analytical model for flow duration curves in seasonally dry climates, Water Resour. Res., 50, 5510–5531, doi:10.1002/2014WR015301, 2014. 9769, 9770, 9772, 9776, 9777, 9778, 9785, 9786, 9793, 9794, 9795, 9802

Müller, M. F., Thompson, S. E., and Kelly, M. N.: Bridging the information gap: a webGIS tool for rural electrification in data-scarce regions, Appl. Energ., in review, 2015. 9767, 9770

Muneepeerakul, R., Azaele, S., Botter, G., Rinaldo, A., and Rodriguez-Iturbe, I.: Daily streamflow analysis based on a two-scaled gamma pulse model, Water Resour. Res., 46, W11546, doi:10.1029/2010WR009286, 2010. 9769

NASA Land Processes Distributed Active Archive Center (LP DAAC): ASTER GDEM v2, NASA Land Processes Distributed Active Archive Center (LP DAAC), ASTER L1 B, USGS/Earth Resources Observation and Science (EROS) Center, Sioux Falls, 2011. 9774

Nathan, R. and McMahon, T.: Evaluation of automated techniques for base flow and recession analyses, Water Resour. Res., 26, 1465–1473, 1990. 9776

Sauquet, E. and Catalogne, C.: Comparison of catchment grouping methods for flow duration curve estimation at ungauged sites in France, Hydrol. Earth Syst. Sci., 15, 2421–2435, doi:10.5194/hess-15-2421-2011, 2011. 9768

Schaefli, B., Rinaldo, A., and Botter, G.: Analytic probability distributions for snow-dominated streamflow, Water Resour. Res., 49, 2701–2713, doi:10.1002/wrcr.20234, 2013. 9769

HESSD
12, 9765–9811, 2015

FDC Predictions in ungauged basins

M. F. Müller and S. E. Thompson

Searcy, J. and Hardison, C.: Double-Mass Curves. Manual of Hydrology: Part I, General Surface Water Techniques, US Geological Survey Water-Supply Paper 1541-B, United States Government Printing Office, Washington, 1960. 9774

Shao, J. and Tu, D.: The Jackknife and Bootstrap, Springer-Verlag, New York, 2012. 9778

Shrestha, D. P.: Assessment of soil erosion in the Nepalese Himalaya: a case study in Likhu Khola Valley, Middle Mountain Region, Land Husbandry, 2, 59–80, 1997. 9777

Stokstad, E.: Scarcity of rain, stream gages threatens forecasts, Science, 285, 1199–1200, doi:10.1126/science.285.5431.1199, 1999. 9767

Thompson, S., Levin, S., and Rodriguez-Iturbe, I.: Linking plant disease risk and precipitation drivers: a dynamical systems framework, Am. Nat., 181, E1–E16, doi:10.1086/668572, 2013a. 9792

Thompson, S. E., Sivapalan, M., Harman, C. J., Srinivasan, V., Hipsey, M. R., Reed, P., Montanari, A., and Blöschl, G.: Developing predictive insight into changing water systems: use-inspired hydrologic science for the Anthropocene, Hydrol. Earth Syst. Sci., 17, 5013–5039, doi:10.5194/hess-17-5013-2013, 2013b. 9770

Turner, A. G. and Annamalai, H.: Climate change and the south Asian summer monsoon, Nature Climate Change, 2, 587–595, doi:10.1038/nclimate1495, 2012. 9780

Turner, A. G. and Slingo, J. M.: Subseasonal extremes of precipitation and active-break cycles of the Indian summer monsoon in a climate-change scenario, Q. J. Roy. Meteor. Soc., 135, 549–567, 2009. 9780, 9783

United States Geological Survey: USGS Threatened and Endangered Streamgages, available at: http://streamstats09.cr.usgs.gov/ThreatenedGages/ThreatenedGages_str.html (last access: 5 August 2015), 2015. 9767

Vogel, R. and Fennessey, N.: Flow-duration curves. I: New interpretation and confidence intervals, J. Water Res. Pl.-ASCE, 120, 485–504, 1994. 9767

HESSD

12, 9765–9811, 2015

FDC Predictions in ungauged basins

M. F. Müller and S. E. Thompson

Table 1. Catchment characteristics. Median values and interquartile distances (IQD) are given for the whole sample of 25 gauges. The table also presents characteristics of the Chepe Kohla watershed considered in the analysis as a case study.

	Streamflow:			Topography:			Climate:							Recession:	
	Q_m	q_{95}	N_y	A	z_m	z_M	P_y	T_{mons}	λ_P	α_P	AR	CV	ET	k	b
All gauges															
– Median	76.1	0.14	22	1355	481	5209	1952	99	0.71	18.8	0.29	0.85	2.5	0.17	2.38
– IQD	106.0	0.06	12	2800	374	4034	1002	7	0.20	7.8	0.09	0.84	1.3	0.08	0.47
Chepe Kohla	23.0	0.14	31	277	475	4711	3050	100	0.84	26.5	0.09	1.03	2.1	0.20	2.41

Q_m is mean annual flow in $m^3 s^{-1}$; q_{95} is the 95th flow percentile normalized by Q_m; N_y indicates the number of observation years; A is the catchment area in km^2; z_m and z_M are respectively the minimum and maximum elevation of the basins meters; P_y is mean precipitation in mm y^{-1}; T_{mons} is the estimated duration of the monsoon in days; λ_P is rainfall frequency during the monsoon (in d^{-1}); α_P is mean rainfall intensity in mm d^{-1}; AR is the first-order autocorrelation coefficient of rainfall occurrence (AR = 0 if rainfall follows a Poissonian process), CV is the coefficient of variation of rainfall intensity on rainy days (CV = 1 if depths are exponentially distributed); ET (mm d^{-1}) is the reference evapotranspiration during the rainy season Lambert and Chitrakar (1989); k is the linear recession constant estimated during the monsoon (in d^{-1}) and b is the non linear exponent of the seasonal recession. A soil moisture capacity of 16 mm are assumed throughout the country (Müller et al., 2014).

HESSD
12, 9765–9811, 2015

FDC Predictions in ungauged basins

M. F. Müller and S. E. Thompson

Table 2. Parameters of the Monte Carlo analysis. At each run, all parameters are drawn independently from a uniform distribution of the specified range.

Characteristic	Description	Distribution range
k^{-1} [d]	Mean response catchment response time during the wet season	[1, 10]
b [–]	Exponent parameter of the seasonal recession	[1, 3]
T_w [d]	Wet season duration	[50, 300]
λ_P^{-1} [d]	Mean inter-arrival time of wet season rainfall	[1, 10]
α_P [mm d^{-1}]	Mean intensity of wet seasonal rainfall	[1, 50]
$\mathrm{Log}_{10}(A)$ [log(km^2)]	(Log) catchment area	[1, 5]
r_{λ_P} [–]	Relative change in rainfall frequency	[−0.9, 0]
r_{α_P} [–]	Relative change in rainfall intensity	[0, 1]

HESSD
12, 9765–9811, 2015
FDC Predictions in ungauged basins
M. F. Müller and S. E. Thompson

Table 3. Linear regression results of the Monte Carlo analysis showing the effect of catchment characteristics on flow resilience. Dependent variables are the Nash–Sutcliffe coefficients estimated between the normalized current and future FDCs obtained from the Monte Carlo analysis. Independent variables are constructed from the randomly drawn catchment characteristics listed in Table 2. The first column presents the raw effects of the catchment characteristics on flow resilience. Column 2–3 test the direction and significance of the effects described in Sect. 4.2.2.

	Dependent variable: Nash–Sutcliffe coefficient		
	(Baseline)	(Wet seas.)	(Dry seas.)
λ_P	$3.17 \times 10^{-1***}$		
	(2.07×10^{-2})		
α_P	$1.49 \times 10^{-3***}$		
	(3.27×10^{-4})		
k	$-4.54 \times 10^{-1***}$		
	(3.32×10^{-2})		
T_w	$-3.23 \times 10^{-4***}$	$-3.36 \times 10^{-4***}$	$-3.68 \times 10^{-4***}$
	(5.72×10^{-5})	(5.70×10^{-5})	(5.81×10^{-5})
b	$-5.75 \times 10^{-2***}$	$-6.14 \times 10^{-2***}$	$-1.02 \times 10^{-1***}$
	(7.46×10^{-3})	(7.42×10^{-3})	(1.21×10^{-2})
λ/k		$6.28 \times 10^{-2***}$	
		(3.19×10^{-3})	
$\lambda_P\alpha_P$			-1.31×10^{-3}
			(2.19×10^{-3})
$\lambda_P\alpha_P{:}b$			$4.06 \times 10^{-3***}$
			(1.03×10^{-3})
Observations	5000	5000	5000
F Statistic	559^{***}	753^{***}	589^{***}

Note: * $p < 0.1$; ** $p < 0.05$; *** $p < 0.01$.

HESSD
12, 9765–9811, 2015

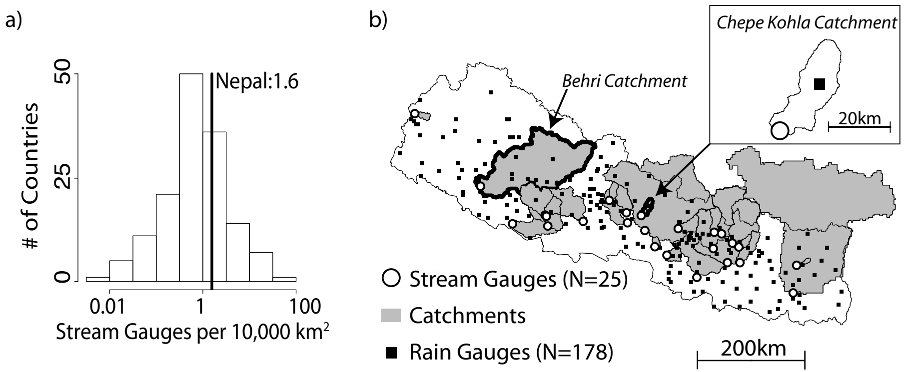

Figure 1. (a) Global histogram of the approximate spatial density of streamflow gauges by nation, represented by the sample of 8540 gauges indexed by the Global Runoff Data Center for 146 countries (Global Runoff Data Center, 2014). With a density of 1.6 gauges $(10\,000\,\mathrm{km}^2)^{-1}$, Nepal falls close to the mode of the global distribution. **(b)** Location of the rain gauges, streamflow gauges and corresponding Nepalese catchments used in the analysis.

HESSD
12, 9765–9811, 2015

FDC Predictions in ungauged basins

M. F. Müller and S. E. Thompson

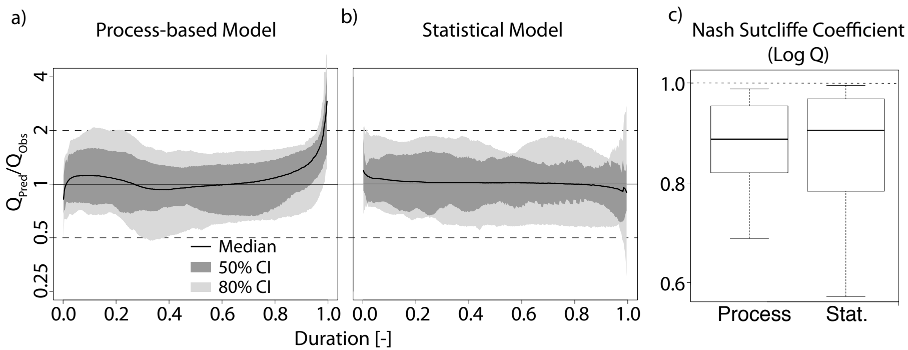

Figure 2. Flow duration curve prediction performance in ungauged basins. The error duration curves of the leave-one-out cross-validation analysis using the process-based and statistical models are presented in panels **(a)** and **(b)** respectively. Relative errors are plotted on a log scale in order to allow the graphs to be balanced on the y axis: a relative prediction error of 2 (the model predicts double the observed value) is at the same distance from $y = 1$ (perfect prediction) than a relative error of 1/2 (the model predicts half the observed value). Durations are plotted on the x axis, with $x = 0$ and $x = 1$ for the highest and lowest flow quantiles respectively. Panel **(c)** shows box plots of Nash–Sutcliffe coefficients computed from log-transformed flow quantiles.

HESSD
12, 9765–9811, 2015

M. F. Müller and S. E. Thompson

Title Page
Abstract | Introduction
Conclusions | References
Tables | Figures
Back | Close
Full Screen / Esc
Printer-friendly Version
Interactive Discussion

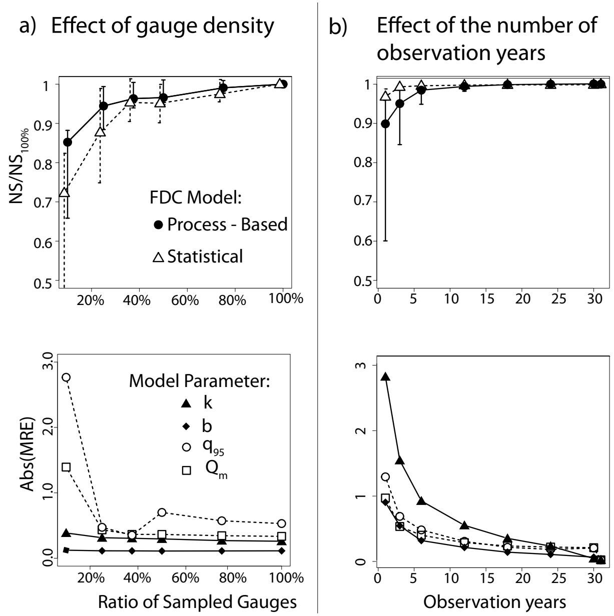

Figure 3. Sensitivity of models to data scarcity. **(a)** Cross-validation analysis showing the sensitivity of both models to a decreasing number of calibration gauges. **(b)** Resampling analysis of streamflow observations in the Chepe Kohla ($N = 10\,000$) catchment showing the effect of the number of observation years. In panels (**a** and **b**), the effects on FDC prediction performances (top) are shown by plotting the ratio of calibration gauges sampled (or the number of observation years) against the relative Nash–Sutcliffe coefficient (with the NSC for the full set of available data as reference). The plot shows the median value for all iterations, and the error bars indicate the interquartile (25–75 %) range. The prediction uncertainties of model parameters (bottom) are given in absolute values of relative prediction errors.

HESSD
12, 9765–9811, 2015

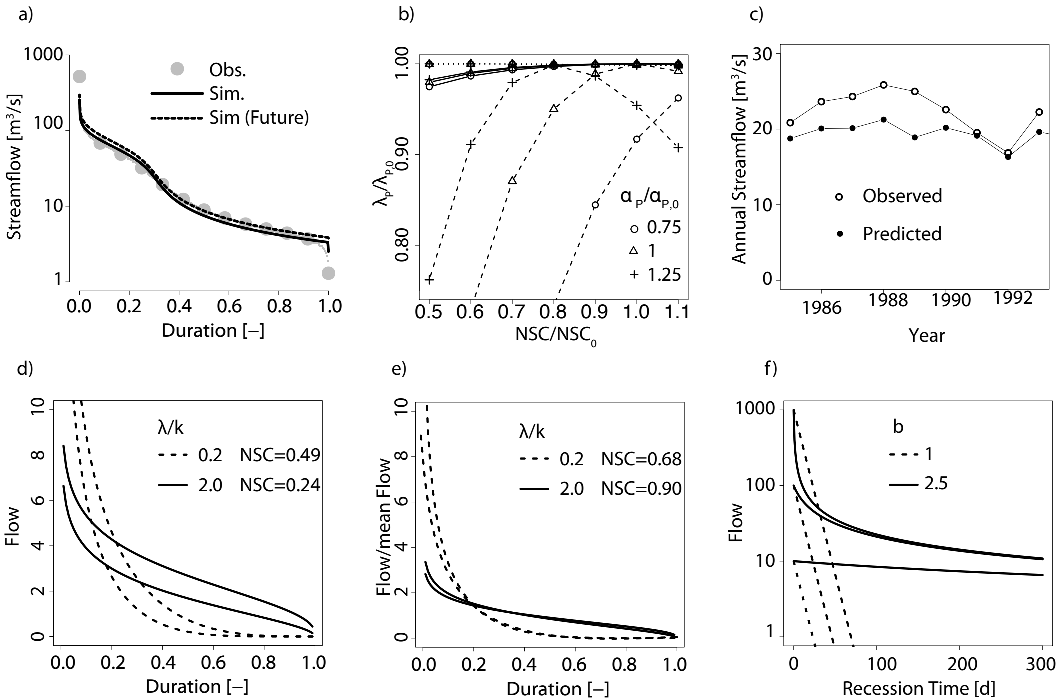

HESSD
12, 9765–9811, 2015

FDC Predictions in ungauged basins

M. F. Müller and S. E. Thompson

Title Page
Abstract | Introduction
Conclusions | References
Tables | Figures
◀| |▶
◀ ▶
Back | Close
Full Screen / Esc
Printer-friendly Version
Interactive Discussion

Figure 4. Sensitivity of models to changes in the precipitation regime. **(a)** Empirical and simulated flow duration curves at Chepe Kohla. The simulated FDC obtained from the stochastic rainfall generator and the bucket watershed model (solid) reproduces the empirical FDC constructed from the observed streamflow well (grey dots). Rainfall changes expected in Nepal ($\alpha_\mathrm{P}/\alpha_{P,0} = 1.2$, $\lambda_\mathrm{P}/\lambda_{P,0} = 0.98$) do not have a substantial influence on the simulated flow distribution (dashed). α_P and λ_P designate the mean depth and frequency of wet season rainfall, respectively. **(b)** Sensitivities to relative changes in rainfall frequency and intensity over the Chepe Kohla catchment. The performance of the process-based model is not affected by rainfall changes (dotted). The sensitivity of the statistical model depends on its ability to predict changes in mean flow from annual rainfall. The model is highly sensitive to rain changes if average streamflow cannot be predicted (dashed), and is robust to moderate changes if average flow is perfectly predicted (solid). **(c)** The model underestimates annual flows at the Chepe Kohla when using a cross-sectional sample (25 gauges) to estimate the local relation between average rainfall and average runoff. **(d)** Effect of a 50 % increase of rainfall frequency on wet-season FDCs for different flow regimes. The persistent regime (solid) is more sensitive to changes than the sporadic regime (dashed), as seen in the lower NSC between "current" and "future" distribution. **(e)** The relationship is inverted when normalizing by mean flow because high flows in the sporadic regime are disproportionately affected by changes in rainfall (dashed). **(f)** Seasonal recessions for linear (dashed) and non-linear (solid) catchments with different initial conditions illustrate that the shape of the recession is affected by initial conditions only if the catchment recessions are non-linear. For identical relative changes in initial conditions (here 1000 %), the effect on recession shape is most important for low initial flow conditions.

HESSD
12, 9765–9811, 2015

M. F. Müller and S. E. Thompson

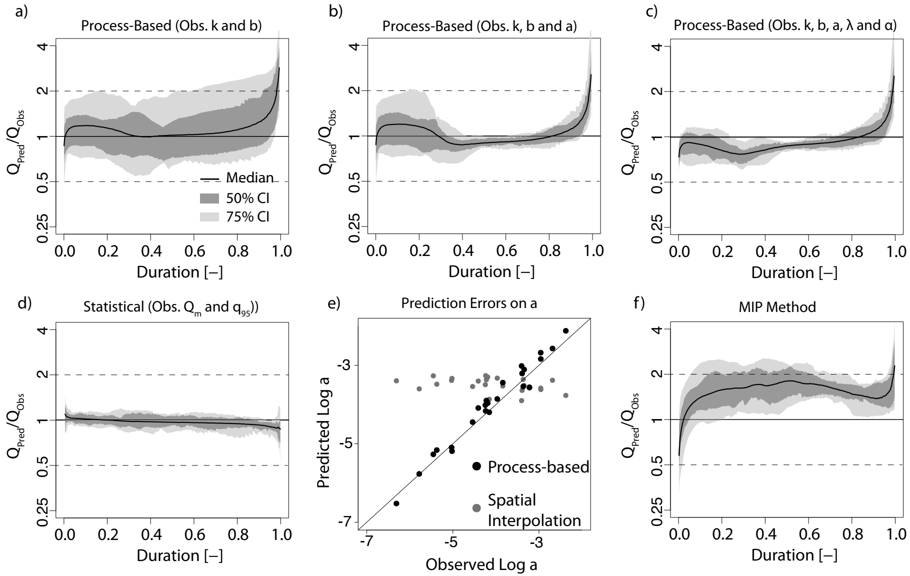

Figure 5. (a–c) Error duration curves illustrating the main sources of prediction uncertainties of the process-based model. **(a)** Errors are marginally affected when using observed values for *k* and *b*, instead of their interpolation from neighboring catchments. **(b)** Errors in low flow decrease substantially when using observed values for *a*, instead of its approximation from *k* and *b* (Eq. 2). **(c)** Errors in high flow decrease substantially when using streamflow, instead of rainfall (see Appendix B), to estimate the frequency λ and mean intensity α of effective rain events. **(e)** Scatterplot of observed vs. predicted values for *a*. Predictions errors are small when using Eq. (2) with observed values of *k* and *b* (black), and significantly larger when interpolating *a* from observed values in neighboring catchments using ordinary kriging (grey). **(f)** Performance in ungauged basins of the MIP method currently used in Nepal for infrastructure design. The method, described in Appendix A, produces significant upward biases on the predicted FDCs.

HESSD
12, 9765–9811, 2015

FDC Predictions in ungauged basins

M. F. Müller and S. E. Thompson

Title Page
Abstract | Introduction
Conclusions | References
Tables | Figures
◀ ▶
Back | Close
Full Screen / Esc
Printer-friendly Version
Interactive Discussion

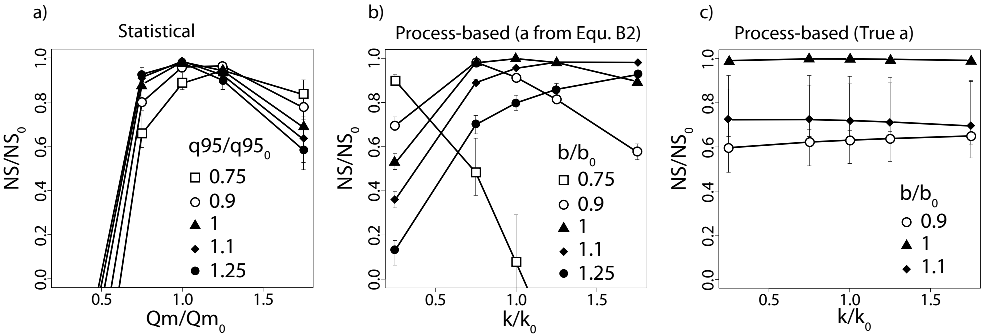

Figure 6. Effect of parameter estimation errors in the predictive performance of the models. Results were obtained using the Monte Carlo analysis described in Appendix C, with errors in the parameters inserted instead of rainfall changes. **(a)** The performance of the statistical model is driven by errors in Q_m, with little effect of q_{95}. **(b)** The process-based model is sensitive to errors in both of its parameters, but k mostly affects prediction performance through its effect on a (Eq. 2). Errors in k have little effect on modeling performance if the true values of a are used instead of Eq. (2) **(c)**.